# Applicability of Macroscopic Transport Models to Decananometer MOSFETs

Martin Vasicek, Johann Cervenka, David Esseni, *Senior Member, IEEE*, Pierpaolo Palestri, *Member, IEEE*, and Tibor Grasser, *Senior Member, IEEE*

***Abstract*—We perform a comparative study of various macroscopic transport models against multisubband Monte Carlo (MC) device simulations for decananometer MOSFETs in an ultrathin body double-gate realization. The transport parameters of the macroscopic models are taken from homogeneous subband MC simulations, thereby implicitly taking surface roughness and quantization effects into account. Our results demonstrate that the drift-diffusion (DD) model predicts accurate drain currents down to channel lengths of about 40 nm but fails to predict the transit frequency below 80 nm. The energy-transport (ET) model, on the other hand, gives good drain currents and transit frequencies down to 80 nm, whereas below 80 nm, the error rapidly increases. The six moments model follows the results of MC simulations down to 30 nm and outperforms the DD and the ET models.**

***Index Terms*—Drift-diffusion (DD) model, energy-transport (ET) model, higher order transport models, quantization, six moments (SM) model, subband Monte Carlo (SMC), surface roughness scattering.**

## I. Introduction

THE fundamental equation describing semiclassical transport is the Boltzmann transport equation (BTE), which has been shown to adequately capture the problem in the absence of quantum mechanical transport effects such as source–drain tunneling. Conventionally, the BTE is solved by some kind of Monte Carlo (MC) approach [1], [2] and more recently by deterministic solution methods employing the spherical harmonics expansion method [3]–[7]. Although solution of the BTE allows for the most detailed consideration of the physics, its high computational effort makes it rather less suitable for engineering applications. However, as the results obtained by these codes are often in good agreement with experiments [8], [9] they are frequently used as a benchmark for simpler models.

Due to the difficulties associated with the solution of the multidimensional BTE, which determines the microscopic distribution function (DF), many simplified macroscopic transport models have been derived [10]–[15]. The simplest and most commonly used macroscopic transport model is the drift-diffusion (DD) model, which comprises the two lowest moments, and it is still the workhorse of today's Technology Computer-Aided Design (TCAD) tools. However, it has been repeatedly discussed and demonstrated that the DD model becomes more and more inaccurate with decreasing device size [16]–[20]. As a consequence, energy-transport (ET) or hydrodynamic[1] models have been suggested, which consider the first three or four moments, most notably some form of average carrier energy [13], [21]. The most severe limitation of these ET models is that they approximate the DF by some form of heated Maxwellian distribution [22], while it is known from MC simulations that the shape of the DF is, in general, more complicated. More details about the DF can be obtained by including additional moments, for instance, the first six [18], [23], [24].

A crucial issue of all macroscopic transport models is the accurate modeling of the transport parameters, for instance, the carrier mobility and energy relaxation time. This is critical, as these transport parameters have to capture all the complex physics that enter the scattering integral of the BTE, such as impurity, phonon, and surface roughness scattering.

Although a number of empirical models for these parameters are available, these models contain "free" parameters, making it tempting to use them as tunable knobs to fit the macroscopic model to experimental or MC data [19], [25]. Unfortunately, the awareness has to be still developed that such a procedure compromises the *consistency* of the models, so that a model tuned in such a way may work just for a particular case and may give unreasonable results otherwise. The simplest example of such an inconsistency is the adjustment of the saturation velocity to account for the missing velocity overshoot in the DD models [19], which makes the model inaccurate in regions with large but nearly homogeneous driving forces.

In order to assess the applicability of macroscopic transport models while guaranteeing their consistency [18], we have previously extracted the transport parameters from homogeneous MC simulations [18], [26]. While this procedure appears suitable for simple $n$-$i$-$n$ structures [18], it is problematic for MOS transistors, where surface roughness scattering and quantization in the inversion layer have a significant impact on the transport parameters. Consequently, in this work, we extract the transport parameters to be set in macroscopic models from an infinitely

Manuscript received July 21, 2011; revised October 6, 2011 and November 14, 2011; accepted December 14, 2011. Date of publication January 27, 2012; date of current version February 23, 2012. The review of this paper was arranged by Editor A. Schenk.

M. Vasicek is with the Wolfgang Pauli Institute, University of Vienna, 1090 Vienna, Austria.

J. Cervenka and T. Grasser are with the Institute for Microelectronics, Vienna University of Technology, 1040 Vienna, Austria.

D. Esseni and P. Palestri are with the Department of Electrical, Mechanical and Management Engineering, University of Udine, 33100 Udine, Italy.

Color versions of one or more of the figures in this paper are available online at http://ieeexplore.ieee.org.

Digital Object Identifier 10.1109/TED.2011.2181177

[1] Although there is considerable ambiguity in literature, we refer to hydrodynamic models strictly as those that retain the convective contributions (e.g., $m\boldsymbol{V}_0^2/2$) to the total carrier energy. Since these models contain hyperbolic terms, they are challenging to solve numerically and therefore never used in TCAD environments.

0018-9383/$31.00 © 2012 IEEE

long homogeneous inversion layer, which is the MOS analog to the uniform bulk case, considering the electronic structure of the 2-D electron gas from a slightly extended version of the multisubband MC solver described in [26]–[30].

In order to show the validity range of the developed models, a practical evaluation is mandatory, which will be given in the next sections.

## II. Review of Macroscopic Models

In this section, the most important steps of the derivations of macroscopic transport models will be reviewed. General conservation and flux equations of the higher order transport models will be explained. Since carrier transport in an inversion layer is based on a 2-D electron gas, a suitable general formulation applicable to different electron dimensionality is chosen [26]. Still, in order to maintain computational efficiency, carrier transport is considered in 3-D $\boldsymbol{k}$-space, whereas the subband structure is incorporated into the models via effective transport parameters. These parameters are chosen such that under homogeneous conditions, the MC results are exactly reproduced.

At an engineering level, a very efficient way to find approximate solutions of the BTE is the method of moments. In order to formulate a set of balance and flux equations, one has to multiply the BTE with a set of weight functions and integrate (average) over $\boldsymbol{k}$-space. An arbitrary number of equations can thus be derived, each containing information from the next higher equation. In order to obtain a tractable model, one has to truncate the equation hierarchy in order to get a fully defined equation set. This assumption to close the system is called "closure relation," which estimates the information of the higher order moments and thus determines the accuracy of the system. For instance, in the case of the DD model, the closure relation for the carriers is assumed to be a drifted Maxwellian distribution [16]. There exist several theoretical approaches that address the closure problem [31], such as the maximum entropy principle in the sense of extended thermodynamics [14], [21], [22], [32]. However, none of them has been found to be of sufficient practical relevance to enter available TCAD codes that rely on rather simple estimates.

To obtain physically meaningful equations, the weight functions $X$ are conventionally chosen as the powers of increasing order of the momentum. Two cases are distinguished depending on whether $X$ is an even scalar-valued function of the wave vector $\boldsymbol{k}$ or an odd vector-valued function of $\boldsymbol{k}$. Multiplying the BTE by the even scalar-valued weights and the odd vector-valued function and then integrating over $\boldsymbol{k}$-space yields the general conservation equation and the general flux equation, respectively.

Using the macroscopic relaxation time approximation for the scattering operator of the BTE, a nonparabolic, isotropic band structure, and a scalar approximation of the tensor valued parameters via their traces, the general conservation equation can be written as

$$\partial_t(nw_l)+\nabla_{\boldsymbol{r}}(n\boldsymbol{V}_l)+l\mathrm{s}_\alpha qn\boldsymbol{V}_{l-1}\nabla_{\boldsymbol{r}}\tilde{\varphi}+n\frac{w_l-w_{l0}}{\tau_l}=0 \quad (1)$$

TABLE I
Transport Parameter Set of the DD, ET, and SM Models: The Carrier Mobility $\mu_0$, the Energy Mobility $\mu_1$, the Second-Order Energy Mobility $\mu_2$, the Energy Relaxation Time $\tau_1$, and the Second-Order Energy Relaxation Time $\tau_2$

| | DD | ET | SM |
|---|---|---|---|
| Mobilities | $\mu_0$ | $\mu_0$, $\mu_1$ | $\mu_0$, $\mu_1$, $\mu_2$ |
| Relaxation Times | | $\tau_1$ | $\tau_1$, $\tau_2$ |

whereas the general flux equation of higher order transport models looks like

$$n\boldsymbol{V}_l=-\frac{n\mu_l}{q}H_{l+1}A\nabla_{\boldsymbol{r}}(nw_{l+1})-s_\alpha n\mu_l(1+lAH_l)w_l\nabla_{\boldsymbol{r}}\tilde{\varphi}. \quad (2)$$

Here, $n$ is the carrier concentration (electrons or holes), $q$ is the elementary charge, $w_l$ is the average energy of the charged carriers defined as $w_l=\langle\mathcal{E}^l\rangle$, $w_{l0}$ is the average equilibrium carrier energy, and $\boldsymbol{V}_l$ denotes the higher order fluxes defined as the velocity times energy $\boldsymbol{V}_l=\langle\boldsymbol{v}\mathcal{E}^l\rangle$, while $\tilde{\varphi}$ is the effective potential. Furthermore, $s_\alpha$ represents a prefix considering the sign of the carrier charge ($s_\alpha=-1$ for electrons and $s_\alpha=+1$ for holes). $H_{l+1}$ is a nonparabolicity factor, whereas $A$ is a dimension factor (in 1DEG: $A=2$, in 2DEG: $A=1$, and in 3DEG: $A=2/3$). The index $l$ denotes the order of the moment. For the DD model, $l$ is equal to 0, whereas for the ET and the six moments (SM) models, $l$ is in the range of $l\in[0,1]$ and $l\in[0,2]$, respectively. $\mu_l$ and $\tau_i$ are the higher order mobility values and relaxation times, which are discussed below.

## III. Modeling of the Transport Parameters

The most general case considered here in terms of transport parameter modeling is the SM model. There, the transport parameters are the carrier mobility $\mu_0$, the energy mobility $\mu_1$, the second-order energy mobility $\mu_2$, the energy relaxation time $\tau_1$, and the second-order energy relaxation time $\tau_2$, which are required to approximate the scattering integral of the BTE and thus have to capture a number of detailed and complex physical processes. Table I summarizes the required transport parameters for each macroscopic model.

### A. *Homogeneous Subband Macroscopic Models*

To include the impact of the inversion layer in the macroscopic models derived above and to characterize high field transport, a model for the mobility values and the relaxation times has been developed, which is based on the parameter extraction from homogeneous subband Monte Carlo (SMC) simulations [26], [33]. Under homogeneous and stationary conditions, the relaxation times can be expressed from (1) as

$$\tau_l=\frac{w_l-w_{l0}}{ls_\alpha qV_{l-1}E} \quad (3)$$

whereas the mobility values can be written as

$$\mu_l=\frac{V_l}{Ew_l(1+lAH_l)} \quad (4)$$

with $E$ as the longitudinal electric field. The energies $w_l$ and $w_{l0}$ as well as the velocity and the nonparabolicity factors $H_1$

and $H_2$ are calculated from the MC simulation in analogy to [18] as

$$H_l = \frac{1}{2w_l} \sum_{i=1}^{d} \langle v_i p_i \mathcal{E}^{l-1} \rangle. \quad (5)$$

Here, $v_i$ and $p_i$ are the velocity and the momentum components with respect to the conduction band minimum of the carriers, respectively. The above formulation guarantees that, under homogeneous conditions, the SMC results, which have been used to create the tables for the transport parameters, are exactly reproduced by the macroscopic transport model. For the ET and SM models, the extracted higher order mobility values and the macroscopic relaxation times are tabulated as a function of average energy and the transverse effective field $E_{\text{eff}}$ defined here as

$$E_{\text{eff}} = \frac{\int_0^{t_{\text{Si}}/2} E_y n dy}{\int_0^{t_{\text{Si}}/2} n dy} \quad (6)$$

where $E_y$ is the electric field perpendicular to the interface, and $t_{\text{Si}}$ is the thickness of our device. In the case of the DD model, the gradient of the quasi-Fermi level is used instead of the average energy [18].

Inversion layer effects such as surface roughness scattering and quantization, which have a considerable impact on the transport parameters, are thus inherently considered in the SMC tables. The higher order transport parameter set from SMC simulations is shown in Fig. 1 for different effective fields of 210 and 950 kV/cm, which demonstrates the considerable impact of the transversal field on the transport parameters.

The extracted higher order transport parameters derived from SMC simulations form the basis for a parameter interpolation within the channel of the device simulator. In the source and in the drain region, the transport parameters are set to their bulk values, which have been extracted from bulk MC simulations as in [34]. The device simulator calculates the transverse effective field in the channel and extracts the mobility values and relaxation times from the SMC tables for the specific device structure. The mobility values and the relaxation times are here independent of the vertical device position. In the DD model, the electric field is used as a parameter, whereas the higher order transport model uses the average energy $w_1$.

For the sake of computational efficiency, quantum mechanical confinement has been considered in the macroscopic device simulator using the improved modified local density approximation (IMLDA) quantum correction model [35], which has been consistently calibrated to the *Schrödinger–Poisson* simulator used in the device SMC (DSMC) simulator.

The most severe limitation of this calculation scheme for the transport parameters is that they do not contain inhomogeneous effects, which are important in all transport parameters since the average energy does not provide a unique parametrization of the DF [15]. Nonetheless, since analytical models suffer from the same limitation, the tabulated parameters give the optimum behavior to be expected from a consistent model.

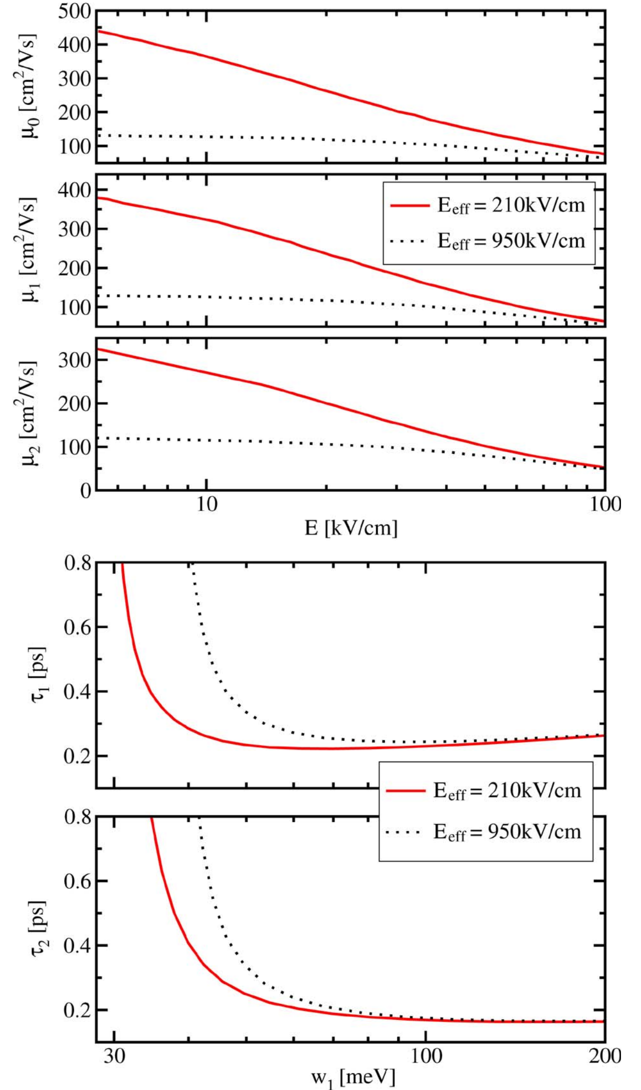


Fig. 1. Homogeneous subband higher order transport parameter defined in Table 1 and extracted from SMC simulations for different effective fields $E_{\text{eff}}$ within a double-gate MOSFET with a thickness of $t_{\text{Si}} = 8$ nm. Note the strong impact of $E_{\text{eff}}$.

To verify the validity of the 2-D macroscopic models, the results are now benchmarked against DSMC simulations. A detailed description of the reference DSMC simulator can be found in [27], [28], and [30].

## IV. Model Evaluation

To compare the performance of these transport models, we simulated a series of double-gate MOSFETs similar to the ones used in [36] and compared the results to the corresponding MC results. The gate length was varied from 1000 nm down to 30 nm with a silicon layer thickness of $t_{\text{Si}} = 8$ nm. To guarantee electrostatic integrity, we used $t_{\text{Si}} = L_{\text{Ch}}/4$ for the channel lengths of 20 and 16 nm. The study of even shorter devices becomes questionable due to the increasing importance of quantum mechanical effects. In order to avoid large temperatures in the contact regions, which lead to artifacts in the

TABLE II
CPU CALCULATION TIMES OF THE COMPLETE OUTPUT CHARACTERISTICS OF A 40- AND A 1000-nm CHANNEL DEVICE (SEE FIGS. 2 AND 3) OF THE DD, ET, AND SM MODELS ARE SHOWN. THE CPU TIME VALUE OF THE DSMC SIMULATOR IS JUST GIVEN FOR ONE BIAS POINT (OP) OF THE OUTPUT CURRENT. IN ALL CASES, THE STATISTICAL ERROR IN THE DRAIN CURRENT IN THE MC SIMULATIONS IS ABOUT 1

| | DD (min) | ET (min) | SM (min) | DSMC (h) |
|---|---|---|---|---|
| $L_{\mathrm{Ch}} = 40\,\mathrm{nm}$ | 3.24 | 5.25 | 16.21 | (OP)≈6 |
| $L_{\mathrm{Ch}} = 1000\,\mathrm{nm}$ | 2.28 | 4.68 | 13.56 | (OP)≈7 |

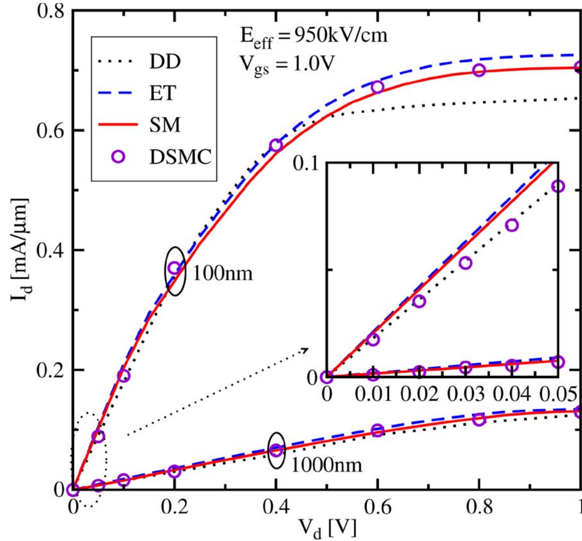


Fig. 2. Output current of 1000- and 100-nm channel devices calculated with the DD, ET, and SM models are compared with the output current obtained from the DSMC simulator. For the 1000-nm device, the results of all models are similar.

macroscopic models due to the cold-Maxwellian boundary conditions, the doping concentration was set to $2 \times 10^{20}$ cm$^{-3}$ in the source/drain regions. The gate/drain biases have been chosen such that the electric field $E$ in all devices was comparable.

The simulation times of the output characteristics of a 40- and a 1000-nm channel length device calculated with the DD, ET, SM, and DSMC models on one core of an Intel Core i7 CPU with 3.4 GHz are summarized in Table II. The simulation time of the DSMC model is shown only for one bias point of the output current in Figs. 2 and 3, respectively. From an efficiency point of view, the macroscopic transport models clearly outperform MC simulations; the accuracy and the validity of each macroscopic transport model will be investigated and discussed in the following sections. In particular, the MC simulation times critically depend on a number of parameters such as the number of particles. Since, for our study, we require accurate reference currents and transit frequencies, the MC simulations were tuned for accuracy rather than speed.

## A. Long-Channel Device

First two long-channel devices with 100 and 1000 nm are simulated to check the consistency of the models. Fig. 2 shows output characteristics calculated with the DD, ET, SM, and DSMC models. For the 1000-nm device, all macroscopic models reproduce the MC reference results, as enforced by the setup of the transport parameters in (3) and (4) very well. For the

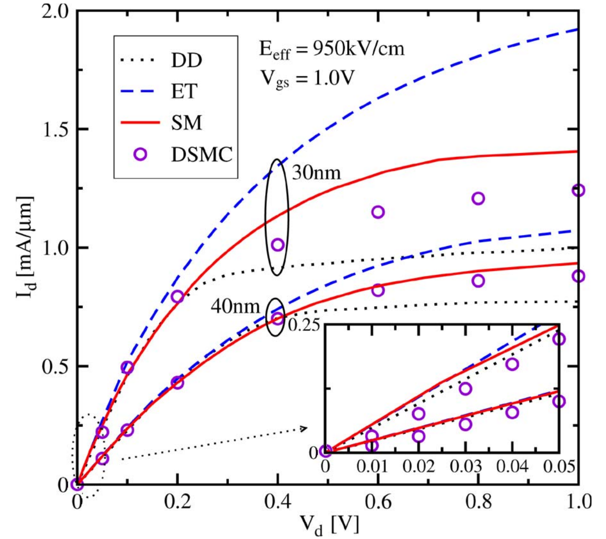


Fig. 3. Output current of a 30- and a 40-nm device using the DD, ET, SM, and DSMC models. The SM model predicts the most accurate result, whereas the ET overestimates and the DD underestimates the current from DSMC simulations.

100-nm channel device, however, the error in the current of the DD and the ET models starts to increase particularly for high drain voltages, whereas the SM model follows the reference DSMC results quite closely. The inset shows the overestimation of the drain current by the ET and SM models in the linear regime, which increases with the reduction in the channel length [37]. The DD model yields lower $I_d$ values, and the ET model slightly overestimates the results from MC simulations. The $I_d$ overestimation of the ET model increases for decreasing channel lengths, as will be shown in the following.

## B. Short-Channel Devices

The simulated drain current of devices with 30- and 40-nm channels is shown in Fig. 3. The inset zooms in the low drain voltage portion of the output characteristics, and we can see that, as known, the macroscopic models overestimate the drain current. Compared with the results obtained from $n-i-n$ structures [37], the overestimation by the macroscopic models appears to be less pronounced. Overall, the SM model yields the most accurate result, whereas the DD model significantly underestimates the results obtained from the DSMC code. On the other hand, the ET model seriously overestimates the maximum drain current. We remark that, just like in the case of the DD model, an improvement in these predictions is possible by adjusting the parameters of the model. In the case of the ET model, it has been observed that the heated and displaced Maxwellian distribution, which is usually employed for the closure relation, results in an overestimation of the heat flux [38]. Similar observations related to the overestimation of the high-energy tail of the DF by a heated Maxwellian distribution have been made in impact ionization models [39] and hot-electron oxide tunneling [40]. As a remedy, it has been suggested to reduce the heat flux of the carrier gas to 10%–20% of its original value [38]. However, the assessment of the general validity of such modifications is beyond the scope of this paper [34].

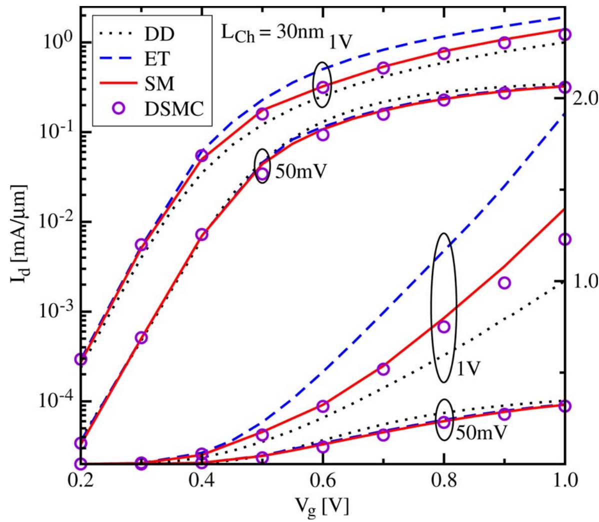


Fig. 4. Transfer characteristics of the 30-nm device for drain voltages of 50 mV and 1 V calculated with the DD, ET, SM, and DSMC models. The macroscopic models overestimate the drain current at low $V_g$, whereas the SM model is particularly accurate at higher voltages.

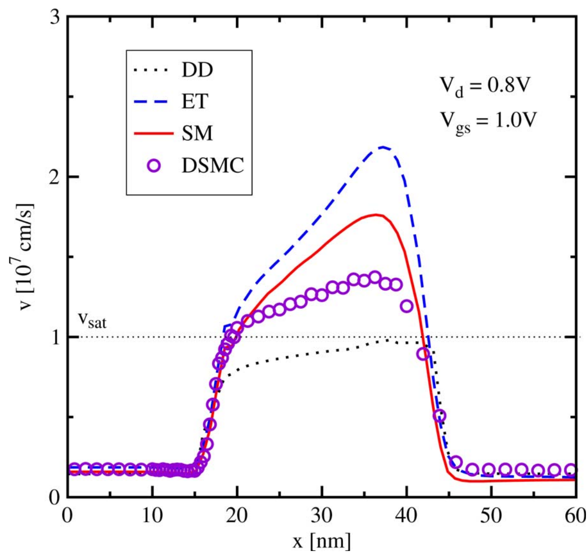


Fig. 5. Velocity profile of a 30-nm-long device calculated with the DD, ET, SM, and DSMC models. A source-to-drain voltage of 0.8 V has been applied. The vertical position of the velocity profile is very close to the interface.

Fig. 4 shows transfer characteristics of the 30-nm device calculated with the DD, ET, SM, and DSMC models for drain voltages of 50 mV and 1 V. The overestimation by macroscopic models at low gate voltages $V_g$ is here more clearly visible.

Fig. 5 presents the velocity profile of the 30-nm-long device. The velocity profile is notoriously difficult to reproduce by macroscopic models and often contains a spurious velocity overshoot at the end of the channel [41]. The ET model clearly overestimates the velocity with respect to the DSMC model, whereas the DD velocity is limited by the saturation velocity. Again, the result closest to the reference DSMC is delivered by the SM model.

Fig. 6 illustrates the relative error in the output current of the macroscopic models as a function of the channel length for the DD, ET, and SM models. For 100 nm, the ET and the SM models yield an output current with an error below 5%, whereas the error in the current of the DD model is about −8%. With a further decrease in the channel length down to 80 nm, the error of the ET model rapidly increases, whereas the SM model stays within 5%. Astonishingly, at about 60 nm, the magnitude of the error of the DD model becomes smaller than that of the ET model. For a critical channel length of 30 nm, the errors of the DD, ET, and SM models are −20%, 54%, and 14%, respectively. The SM model is thus the most accurate model. However, below 30 nm, the results obtained by macroscopic models become questionable. For instance, at a channel length of 16 nm, the errors of the DD, ET, and SM models are −33%, 127%, and 42%, respectively.

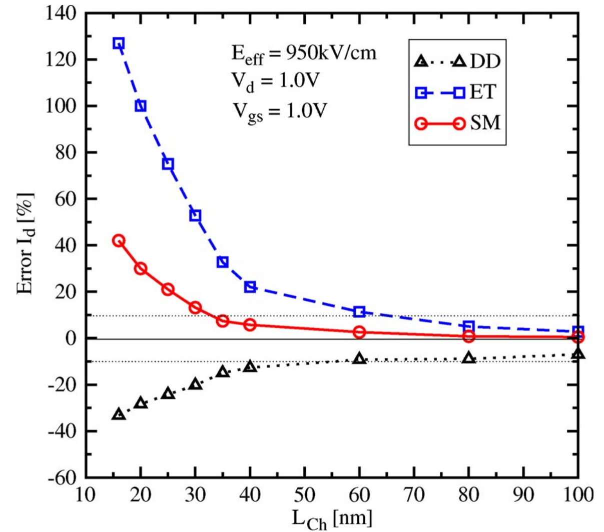


Fig. 6. Relative error in the maximum drain current as a function of the channel length for the DD, ET, and SM models relative to the DSMC results. The error of the ET model rapidly increases for devices with a channel length below 80 nm, where even the DD model shows lower errors. The SM model is the most accurate model for short-channel devices. The ±10% error bounds are indicated by the dotted lines.

It is interesting to note that the error of the DD current is relatively small. This has been explained as a consequence of error cancelation: While the velocity is underestimated, the zero-field conductivity is overestimated [9], [37], [42] (see Figs. 2 and 3). No such error cancelation occurs when other figures-of-merit are considered such as the transit frequencies. Fig. 7 shows the error of the transit frequencies as a function of the channel length. The transit frequencies have been calculated following [9], which requires an accurate velocity profile in the channel but otherwise no additional parameters. We first see that the SM model provides results very close to the reference DSMC simulation down to about 30 nm. In the DD model, the error in $f_T$ is much more severe than the one in $I_d$ (see Fig. 6) due to the lower velocity in the channel (see Fig. 5). Better agreement between MC and DD is usually enforced by modifying the saturation velocity $v_{\mathrm{sat}}$ employed in the mobility model, which then introduces errors at different channel lengths [43]. However, in a consistent model valid for all channel lengths, the SM approach yields the best results and outperforms the ET and the DD models.

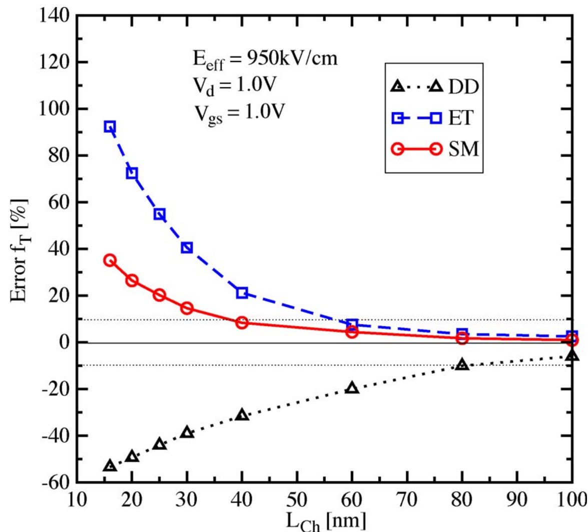


Fig. 7. Relative error in the transit frequencies of the DD, ET, and SM models compared with the DSMC results as a function of the channel length. The error of the DD model is now significantly higher than the error in the maximum drain current (see Fig. 6), whereas the SM model remains the most accurate model.

## V. Conclusion

In order to efficiently describe carrier transport in future device structures, various macroscopic transport models have been proposed over the years. We provide a guideline for the validity of the most prominent macroscopic models, namely, the DD, the ET, and the SM models. To characterize carrier transport in the inversion layer, we use a subband-based macroscopic transport model, where quantum effects as well as surface roughness scattering are inherently included using effective transport parameters. Since we are still in a scattering dominating regime, we neglect quantum effects in transport direction expected to become important only for $L_{\mathrm{Ch}} \leq 6$ nm [44]. As reference, we took data from DSMC simulations.

Overall, the DD model is found to be reasonably accurate for devices with a channel length of at least 100 nm. The ET model, on the other hand, remains valid down to 80 nm. Curiously, below 80 nm, the ET model loses its validity and gives larger errors in the drain current than the DD model. Finally, the SM model is accurate throughout the whole channel length investigation down to 30 nm. The final limit of this model appears to be around 30 nm, as also stated for the bulk case in [18] and [34]. Below that channel length, the results predicted by macroscopic transport models should be considered with a reasonable amount of suspicion.

## References


[1] C. Jungemann, S. Keith, M. Bartels, and B. Meinerzhagen, "Efficient full-band Monte Carlo simulation of silicon devices," *IEICE Trans. Electron*, vol. E82-C, no. 6, pp. 870–879, Jun. 1999.

[2] F. Bufler, Y. Asahi, H. Yoshimura, C. Zechner, A. Schenk, and W. Fichtner, "Monte Carlo simulation and measurement of nanoscale n-MOSFETs," *IEEE Trans. Electron Devices*, vol. 50, no. 2, pp. 418–424, Feb. 2003.

[3] C. Jungemann, A. Pham, and B. Meinerzhagen, "Stable discretization of the Boltzmann equation based on spherical harmonics, box integration, and a maximum entropy dissipation principle," *J. Appl. Phys.*, vol. 100, no. 2, p. 024 502, Jul. 2006.

[4] T. Tang and H. Gan, "Two formulations of semiconductor transport equations based on spherical harmonic expansion of the Boltzmann transport equation," *IEEE Trans. Electron Devices*, vol. 47, no. 9, pp. 1726–1732, Sep. 2000.

[5] K. Rupp, A. Jüngel, and T. Grasser, "Matrix compression for spherical harmonics expansions of the Boltzmann transport equation for semiconductors," *J. Comput. Electron.*, vol. 229, no. 23, pp. 8750–8765, Nov. 2010.

[6] M. Lenzi, P. Palestri, E. Gnani, S. Reggiani, A. Gnudi, D. Esseni, L. Selmi, and G. Baccarani, "Investigation of the transport properties of silicon nanowires using deterministic and Monte Carlo approaches to the solution of the Boltzmann transport equation," *IEEE Trans. Electron Devices*, vol. 55, no. 8, pp. 2086–2096, Aug. 2008.

[7] K. Banoo, M. Lundstrom, and R. Smith, "Direct solution of the Boltzmann transport equation in nanoscale Si devices," in *Proc. Simul. Semicond. Process. Devices*, 2000, pp. 50–53.

[8] C. Jacoboni and L. Reggiani, "The Monte Carlo method for the solution of charge transport in semiconductors with applications to covalent materials," *Rev. Mod. Phys.*, vol. 55, no. 3, pp. 645–705, Jul.–Sep. 1983.

[9] C. Jungemann and B. Meinerzhagen, *Hierachical Device Simulation The Monte Carlo Perspective*, S. Selberherr, Ed. New York: Springer-Verlag, 2003.

[10] R. Stratton, "Diffusion of hot and cold electrons in semiconductor barriers," *Phys. Rev.*, vol. 126, no. 6, pp. 2002–2014, Jun. 1962.

[11] K. Blotekjaer, "Transport equations for electrons in two-valley semiconductors," *IEEE Trans. Electron Devices*, vol. ED-17, no. 1, pp. 38–47, Jan. 1970.

[12] A. Anile and O. Muscato, "Improved hydrodynamic model for carrier transport in semiconductor," *Phys. Rev. B*, vol. 51, pp. 728–740, 1995.

[13] R. Thoma, A. Emunds, B. Meinerzhagen, H. Peifer, and W. Engl, "Hydrodynamic equations for semiconductors with nonparabolic band structure," *IEEE Trans. Electron Devices*, vol. 38, no. 6, pp. 1343–1353, Jun. 1991.

[14] O. Muscato and V. Romano, "Simulation of submicron silicon diodes with a non-parabolic hydrodynamical model based on the maximum entropy principle," in *Proc. 7th Int. Workshop Book Abstracts Comput. Electron. IWCE Glasgow*, May 22–25, 2000, pp. 94–95.

[15] T. Grasser, T. Tang, H. Kosina, and S. Selberherr, "A review of hydrodynamic and energy-transport models for semiconductor device simulation," *Proc. IEEE*, vol. 91, no. 2, pp. 251–274, Feb. 2003.

[16] M. Lundstrom, *Fundamentals of Carrier Transport.*. Cambridge, U.K.: Cambridge Univ. Press, 2000.

[17] A. Abramo, L. Baudry, R. Brunetti, R. Castagne, M. Charef, F. Dessenne, P. Dollfus, R. Dutton, W. L. Engl, R. Fauquembergue, C. Fiegna, M. V. Fischetti, S. Galdin, N. Goldsman, M. Hackel, C. Hamaguchi, K. Hess, K. Hennacy, P. Hesto, J. M. Higman, T. Iizuka, C. Jungemann, Y. Kamakura, H. Kosina, T. Kunikiyo, S. E. Laux, C. Maziar, H. Mizuno, H. J. Peifer, S. Ramaswamy, N. Sano, P. G. Scrobohaci, S. Selberherr, M. Takenaka, K. Taniguchi, J. L. Thobel, R. Thoma, K. Tomizawa, M. Tomizawa, T. Vogelsang, S.-L. Wang, X. Wang, C.-S. Yao, P. D. Yoder, and A. Yoshii, "A comparison of numerical solutions of the Boltzmann transport equation for high-energy electron transport silicon," *IEEE Trans. Electron Devices*, vol. 41, no. 9, pp. 1646–1654, Sep. 1994.

[18] T. Grasser, R. Kosik, C. Jungemann, H. Kosina, and S. Selberherr, "Non-parabolic macroscopic transport models for device simulation based on bulk Monte Carlo data," *J. Appl. Phys.*, vol. 97, no. 9, p. 093 710, May 2005.

[19] J. Bude, "MOSFET modeling into the ballistic regime," in *Proc. Simul. Semicond. Process. Devices*, Seattle, WA, Sep. 2000, pp. 23–26.

[20] W. Hänsch and M. Mattausch, "The hot electron problem in small semiconductor devices," *J. Appl. Phys.*, vol. 60, no. 2, pp. 650–656, Jul. 1986.

[21] A. Anile and S. Pennisi, "Extended thermodynamics of the Blotekjaer hydrodynamical model for semiconductors," *Continuum Mech. Thermodyn.*, vol. 4, no. 3, pp. 187–197, Sep. 1992.

[22] T. Grasser, "Non-parabolic macroscopic transport models for semiconductor device simulation," *Phys. A*, vol. 349, no. 1/2, pp. 221–258, Apr. 2005.

[23] T. Grasser, H. Kosina, M. Gritsch, and S. Selberherr, "Using six moments of Boltzmann's transport equation for device simulation," *J. Appl. Phys.*, vol. 90, no. 5, pp. 2389–2396, Sep. 2001.

[24] T. Grasser, H. Kosina, C. Heitzinger, and S. Selberherr, "Characterization of the hot electron distribution function using six moments," *J. Appl. Phys.*, vol. 91, no. 6, pp. 3869–3879, Mar. 2002.

[25] T. Tang, "Hydrodynamic transport modeling of semiconductor devices—Issues and some solutions," in *Proc. Semicond. TCAD Workshop Exhib.*, Hsinchu, Taiwan, May 1999, pp. 1–19.

[26] M. Vasicek, J. Cervenka, M. Wagner, M. Karner, and T. Grasser, "A 2D non-parabolic six-moments model," *Solid State Electron.*, vol. 52, no. 10, pp. 1606–1609, Oct. 2008.

[27] L. Lucci, D. Esseni, P. Palestri, and L. Selmi, "Comparative analysis of basic transport properties in the inversion layer of bulk and SOI

MOSFETs: A Monte-Carlo study," in *Proc. 34th ESSDERC*, Sep. 21–23, 2004, pp. 321–324.
[28] L. Lucci, P. Palestri, D. Esseni, and L. Selmi, "Multi-subband Monte Carlo modeling of nano-MOSFETs with strong vertical quantization and electron gas degeneration," in *IEDM Tech. Dig.*, 2005, pp. 631–634.
[29] P. Palestri, R. Clerc, D. Esseni, L. Lucci, and L. Selmi, "Multi-subband-Monte-Carlo investigation of the mean free path and of the kT layer in degenerated quasi ballistic nano MOSFETs," in *IEDM Tech. Dig.*, Dec. 11–13, 2006, pp. 945–948.
[30] L. Lucci, P. Palestri, D. Esseni, L. Bergagnini, and L. Selmi, "Multisubband Monte Carlo study of transport, quantization, and electron-gas degeneration in ultrathin SOI n-MOSFETs," *IEEE Trans. Electron Devices*, vol. 54, no. 5, pp. 1156–1164, May 2007.
[31] C. Levermore, "Moment closure hierarchies for kinetic theories," *J. Stat. Phys.*, vol. 83, no. 5/6, pp. 1021–1065, Jun. 1996.
[32] A. Anile, W. Allegretto, and C. Ringhofer, *Mathematical Problems in Semiconductor Physics*. New York: Springer-Verlag, 1988.
[33] M. Vasicek, J. Cervenka, M. Wagner, M. Karner, and T. Grasser, "Parameter modeling for higher-order transport models in UTB SOI MOSFETs," *J. Comput. Electron.*, vol. 7, no. 3, pp. 168–171, Sep. 2008.
[34] T. Grasser, C. Jungemann, H. Kosina, B. Meinerzhagen, and S. Selberherr, "Advanced transport models for sub-micrometer devices," in *Proc. Simul. Semicond. Process. Devices*, 2004, pp. 1–8.
[35] C. Jungemann, C. Nguyen, B. Neinhüs, S. Decker, and B. Meinerzhagen, "Improved modified local density approximation for modeling of size quantization in NMOSFETs," in *Proc. Int. Conf. Model. Simul. Microsyst.*, 2001, pp. 458–461.
[36] F. Bufler, A. Schenk, and W. Fichtner, "Monte Carlo, hydrodynamic and drift-diffusion simulation of scaled double-gate MOSFETs," *J. Comput. Electron.*, vol. 2, pp. 81–84, 2003.
[37] C. Jungemann, T. Grasser, B. Neinhüs, and B. Meinerzhagen, "Failure of moments-based transport models in nanoscale devices near equilibrium," *IEEE Trans. Electron Devices*, vol. 52, no. 11, pp. 2404–2408, Nov. 2005.
[38] I. Bork, C. Jungemann, B. Meinerzhagen, and W. Engl, "Influence of heat flux on the accuracy of hydrodynamic models for ultra-short Si MOSFETs," in *Proc. Int. Workshop NUPAD V*, Honolulu, HI, 1994, pp. 63–66.
[39] T. Grasser, H. Kosina, and S. Selberherr, "Influence of the distribution function shape and the band structure on impact ionization modeling," *J. Appl. Phys.*, vol. 90, no. 12, pp. 6165–6171, Dec. 2001.
[40] A. Gehring, T. Grasser, H. Kosina, and S. Selberherr, "Simulation of hot-electron oxide tunneling current based on a non-Maxwellian electron energy distribution function," *J. Appl. Phys.*, vol. 92, no. 10, pp. 6019–6027, Nov. 2002.
[41] T. Grasser, H. Kosina, and S. Selberherr, "Investigation of spurious velocity overshoot using Monte Carlo data," *J. Appl. Phys. Lett.*, vol. 79, no. 12, pp. 1900–1903, Sep. 2001.
[42] M. Zilli, D. Esseni, P. Palestri, and L. Selmi, "On the apparent mobility in nanometric n-MOSFETs," *IEEE Electron Device Lett.*, vol. 28, no. 11, pp. 1036–1039, Nov. 2007.
[43] J. Bude, "MOSFET modeling into the ballistic regime," in *Proc. Simul. Semicond. Process. Devices*, 2000, pp. 50–53.
[44] P. Dollfus, D. Querlioz, J. Saint-Martin, V. Do, and A. Bournel, "Wigner Monte Carlo approach to quantum transport in nanodevices," in *Proc. Simul. Semicond. Process. Devices*, 2008, pp. 277–280.

**Martin Vasicek** was born in Vienna, Austria, in 1979. He received the Dipl.-Ing. degree in physics and the Ph.D. degree from Vienna University of Technology, Vienna, Austria, in 2005 and 2009, respectively.

Since January 2010, he has been a Postdoctoral Researcher with the Wolfgang Pauli Institute, Vienna University, Vienna. His research interests include higher order macroscopic transport models for advanced semiconductor devices and the computational modeling of nanowire field effect transistor and gas sensors.

**Johann Cervenka** was born in Schwarzach, Austria, in 1968. He received the Dipl.-Ing. degree in electrical engineering and the Ph.D. degree in technical sciences from Vienna University of Technology, Vienna, Austria, in 1999 and 2004, respectively.

In November 1999, he joined the Institute for Microelectronics, Vienna University of Technology. His scientific interests include 3-D mesh generation, and algorithms and data structures in computational geometry.

**David Esseni** (S'98–M'00–SM'06) received the Laurea and Ph.D. degrees in electronic engineering from the University of Bologna, Bologna, Italy.

In 2000, he was a Visiting Scientist with Bell Labs, Lucent Technologies, Murray Hill, NJ. He is currently an Associate Professor with the University of Udine, Udine, Italy. His research interests include the characterization, modeling, and reliability of MOS transistors and non-volatile memory (NVM) devices. In the field of NVM, he has worked on the low-voltage and substrate-enhanced hot-electron phenomena and on several aspects of Flash memory devices. In the framework of CMOS technologies, he has been involved in several activities concerning experimental characterization and modeling of mobility in silicon, strained silicon, and germanium transistors with both planar and innovative device architectures. He is a coauthor of the book *Nanoscale MOS transistors: Semi-Classical Transport and Application* (Cambridge: Cambridge University Press, 2011) and of several book chapters and of numerous papers in his fields of expertise. His curent research interests include beyond-CMOS devices, such as graphene-based and tunnel field-effect transistors, and quantum transport in nonequilibrium Green's function formalism.

Dr. Esseni has served or is serving as a member of the technical committee of the International Electron Devices Meeting, the European Solid-State Device Research Conference, and the International Reliability Physics. He is an Associate Editor of the IEEE TRANSACTIONS ON ELECTRON DEVICES (IEEE-TED) and has been a Co-Guest Editor of two special issues of the IEEE-TED focused respectively on the simulation and modeling of nanoelectronic devices and to the characterization and modeling of the variability.

**Pierpaolo Palestri** (M'05) received the Laurea degree in electronic engineering from the University of Bologna, Bologna, Italy, in 1998, and the Ph.D. degree in electronic engineering from the University of Udine, Udine, Italy, in 2003.

In 1998, he joined the Department of Electrical, Mechanical and Management Engineering, University of Udine as a Research Assistant in the field of device simulation. From July 2000 to September 2001, he held a postdoctoral position with Bell Laboratories, Lucent Technologies (now Agere Systems), Murray Hill, NJ, where he worked on high-speed silicon-germanium bipolar technologies. In October 2001, he became an Assistant Professor, and in November 2005, he became an Associate Professor with the University of Udine. He is the author or coauthor of more than 150 papers in refereed journals and conference proceedings. His research interests include the modeling of carrier transport in nanoscale devices, and the simulation of hot-carrier and tunneling phenomena in scaled MOSFETs and nonvolatile memory cells.

Dr. Palestri has served as a Technical Program Committee Member for the International Electron Devices Meeting in 2008 and 2009.

**Tibor Grasser** (SM'05) received the Dipl.-Ing. degree in communications engineering, the Ph.D. degree in technical sciences, and the *Venia Docendi* in microelectronics from the Vienna University of Technology in 1995, 1999, and 2002, respectively.

Since 1997, he has been the Head of the Minimos-NT Development Group, working on the successor of the highly successful MiniMOS program. He was a visiting Research Engineer with Hitachi Ltd., Tokyo, Japan, and for the Alpha Development Group, Compaq Computer Corporation, Shrewsbury, MA. From 2003 to 2010, he was the Director of the Christian Doppler Laboratory for technology computer-aided design in microelectronics. He is currently employed as an Associate Professor with the Institute for Microelectronics, Vienna University of Technology. He is the author or coauthor of over 300 articles in scientific books, journals, and conferences proceedings, and has presented invited talks, tutorials and short courses at various conferences such as the International Electron Devices Meeting (IEDM), International Reliability Physics Symposium (IRPS), The International Conference on Simulation of Semiconductor Processes and Devices (SISPAD), European Solid-State Device Research Conference (ESSDERC), IEEE International Integrated Reliability Workshop (IIRW), European Symposium on Reliability of Electron Devices, Failure Physics and Analysis (ESREF), Insulating Films on Semiconductors (INFOS), International Semiconductor Device Research Symposium (ISDRS), and the Electrochemical Society (ECS) meetings. He is also an Editor of a book on advanced device simulation and organic electronics. His current research interests include semiconductor device reliability issues and device modeling in general.

Dr. Grasser is a Distinguished Lecturer of the IEEE Electron Devices Society and has been involved in the program committees of conferences such as IEDM, IRPS, SISPAD, IWCE, ESSDERC, IIRW, and ISDRS. He was also the Chair of SISPAD 2007. He was a recipient of the Best Paper Awards at IRPS (2008 and 2010) and ESREF 2008.